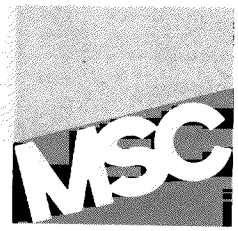

THE MACNEAL-SCHWENDLER CORPORATION
815 Colorado Boulevard Los Angeles, California 90041
Tel: (213) 258-9111 • TWX: 910 321-2492 • Telex: 4720462

PRESSURE FOLLOWER MATRIX FOR GEOMETRIC NONLINEAR FINITE ELEMENT ANALYSIS

A paper presented at the
1987 MSC/NASTRAN User's Conference

by

David N. Herting
Gernot W. Haggenmacher

March 1987

PRESSURE FOLLOWER MATRIX
FOR
GEOMETRIC NONLINEAR FINITE ELEMENT ANALYSIS

David N. Herting* and Gernot W. Haggenmacher**

ABSTRACT

The variation of pressure loads due to displacement variations in nonlinear geometric analysis is developed in terms of a tangent finite element matrix. This so-called follower force matrix is significant relative to the normal geometric tangent matrices for many problems and improves the convergence of the nonlinear solution. The effects of the follower force matrices are also important for analyzing problems of instabilities and dynamics under pressure, such as containers and tires where an accurate tangent matrix is required. Special finite elements are implemented in MSC/NASTRAN to represent the tangent stiffness of pressure loads on surfaces. Results shown for buckling solutions and normal mode analysis, indicate dramatic improvement in the results.

INTRODUCTION

Externally applied loads are included in the force equilibrium equations in all finite element structural analysis codes. The nonlinear effects of "follower forces", which change direction and magnitude with large element motions are included as direct force updates in most nonlinear analysis codes. However, the tangent stiffness terms generated by follower forces are rarely included. A recent paper (Ref. 1.) shows the difficulties in defining the general forms of the follower force matrices. The development below is an attempt to simplify these ideas.

* Vice President of Engineering
The MacNeal-Schwendler Corporation

** Private Consultant
Finite Element Technology

The tangent stiffness effects of "follower forces" are usually ignored for direct nonlinear static or transient response problems. The modified Newton methods and explicit integration systems used to find solutions do not require exact tangent matrices to obtain accurate answers. The tangent stiffness of the finite elements themselves is usually sufficient to provide reasonable approximations for the search algorithm. However, in special problems involving shells under pressure, such as automobile tires and wind sails, the convergence rate of the Newton methods have been very poor.

Other indirect solutions require more precise tangent properties than are presently included in the conventional "geometric stiffness" or "differential stiffness" matrices. Changes in tangent matrices are used in buckling analysis to predict unstable or bifurcation points. Dynamicists frequently use the nonlinear static (preload) solution as a reference state for modal studies or frequency analysis where small motions are assured.

In the development described below a special set of finite element terms are derived for the case of pressure loads for line elements, triangular surface elements and quadrilateral surface elements. These matrices have very interesting properties that result in symmetric, conservative systems under certain special conditions but remain unsymmetric for the general case. Also included are example problems that illustrate the importance of these effects.

THEORETICAL BACKGROUND

Linear methods of Finite Element Analysis evolve naturally into geometrically nonlinear forms when consistent principles and coordinate systems are applied. Variational methods applied to virtual work equations lead to equilibrium equations which lead to matrix solution methods.

For large geometry changes in the MSC/NASTRAN systems the so-called "Updated Lagrangian" method is used to account for the changes in orientation of the materials and finite elements. The stresses and strains in the moving material coordinates produce potential elastic energy which is minimized by the variational method. The changes in the external load vectors produce a corresponding work term which may also be included in the variational process to produce the generalized forces.

The virtual work principle is used to develop the basic finite element equations. A basic static form taken from Ref. [2] is:

$$\delta\Psi = \int_V \sigma\ \delta\varepsilon\ dV - \int_V \vec{b}\cdot\delta\vec{u}\ dV - \int_\Gamma \vec{t}\cdot\delta\vec{u}\ d\Gamma \tag{1}$$

where
- $\delta\Psi$ is the variation of virtual work
- dV is an incremental volume
- $d\Gamma$ is an incremental exterior surface
- σ is the stress tensor at a point
- $\delta\varepsilon$ are the variation of infinitesimal strains
- $\vec{b}$ is the applied body force vector at a point
- $\vec{t}$ is the applied surface force vector at a point
- $\delta\vec{u}$ is the variation of the displacement vector at a point

The first term on the right hand side is used to develop the familiar finite element forces and matrices. In this paper we will concentrate on the last term, namely the work caused by external pressures. First we must convert the integral equation to finite element matrices.

In order to develop finite element matrix terms we make the following definitions:

$$\delta\vec{u}(x, y, z) = \vec{N}_i(x, y, z)\delta u_i \tag{2}$$

where $\vec{N}_i$ is the value of the finite element shape function corresponding to a particular grid point displacement attached to the element and δu_i is the variation of the grid point displacements. In the present case $\vec{N}_i$ are the motions of a surface.

For scalar pressure loads, p, we may replace the scalar surface increment, $d\Gamma$, with the surface vector increment, $d\vec{S}$, where

$$\vec{t}\ d\Gamma = -p d\vec{S} \tag{3}$$

Note that the vector $d\vec{S}$ faces outward on the finite element, and will move and rotate with large motions. However, in the case investigated the pressure also moves with the element or "follows" the structure.

For a single finite element surface, S, the variational work due to pressure is obtained by combining Eqs. (2) and (3) with the last terms of Eq. (1), $\delta\psi^p$, which results in:

$$\delta\psi^p = \int_S p\ \delta u_i\ \vec{N}_i \cdot d\vec{S} \tag{4}$$

The force vector is therefore:

$$F_i^p = \frac{\partial(\delta\psi^p)}{\partial(\delta u)} = \int_S p\ \vec{N}_i \cdot d\vec{S} \tag{5}$$

However, the surface S changes shape and direction with large finite element motions. MSC/NASTRAN accounts for these changes by calculating new F_i vectors during the iteration cycle.

For a true "tangent matrix" we may also examine the derivatives of F_i^p. Taking derivatives with respect to a generalized displacement, u_j, we obtain the tangent terms, K_{ij}^p, due to pressure as:

$$K_{ij}^p = \frac{\partial F_i^p}{\partial u_j} = \frac{\partial}{\partial u_j} \int_S p\ \vec{N}_i \cdot d\vec{S} \tag{6}$$

Note that for the general case the system will be unsymmetric. For higher order elements it is expected that both the surface and the shape functions will change with displacements. However, for the simple linear elements the integral may be simplified as shown in the following examples.

Pressure Follower Loads on Line Element

The simplicity of line elements in a two-dimensional space is well suited to observe and dervive the basic principles of pressure follower loads and the corresponding follower load stiffness matrix. In the subsequent section it will then be developed for surface elements.

a) Basic Forces

The basic geometry for a line element is shown in Figure 1.

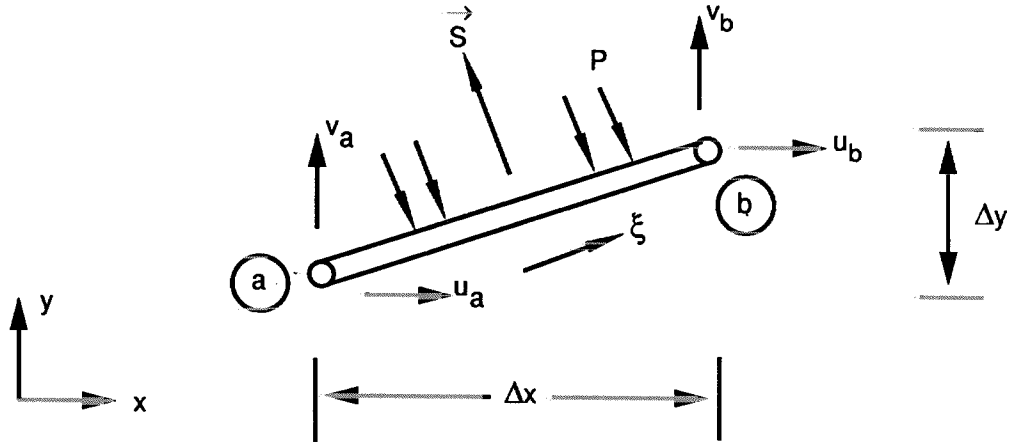

Figure 1. Line Element Geometry.

The surface vector (for a unit width) is:

$$\vec{S} = -\Delta y\ \vec{i} + \Delta x\ \vec{j} \tag{7}$$

Also note that for an increment of the isoparametric variable, ξ

$$d\vec{S} = \left(-\Delta y\vec{i} + \Delta x\vec{j}\right)d\xi \tag{8}$$

The shape functions are:

$$\vec{N}_{ax} = (1 - \xi)\vec{i} \qquad \vec{N}_{ay} = (1 - \xi)\vec{j}$$
$$\vec{N}_{bx} = \xi\,\vec{i} \qquad \vec{N}_{by} = \xi\,\vec{j} \tag{9}$$

where ξ is the dimensionless length parameter.

The forces are obtained by substituting Eqs. (8) and (9) into Eq. (3).

For example:

$$F_{ax} = \int_S p\,\vec{N}_{ax}\cdot d\vec{S} = p\int_0^1 (1 - \zeta)(-\Delta y)d\zeta = -\frac{1}{2}\,p\Delta y \tag{10}$$

Also

$$F_{ay} = \frac{1}{2}\,p\Delta x \tag{11}$$

$$F_{bx} = -\frac{1}{2}\,p\Delta y \tag{12}$$

$$F_{by} = \frac{1}{2}\,p\Delta x \tag{13}$$

Note that if Δx and Δy are updated with new displacements the forces also are updated. For tangent stiffness matrix effects we may take the derivatives of the forces with respect to the motions.

b) Stiffness Matrix

For the stiffness matrix we must include the effect of displacements on the geometry, i.e.:

$$\Delta x = \Delta x^r + u_b - u_a \tag{14}$$

$$\Delta y = \Delta y^r + v_b - v_a \tag{15}$$

where Δx^r and Δy^r are measured at the reference state (u = 0).

From Eq. (6), the stiffness matrix terms are:

$$K^{p}_{ij} = - \frac{\partial F_i}{\partial u_j} = \int_S p \, \vec{N}_i \cdot \frac{\partial (\vec{dS})}{\partial u_j} \tag{16}$$

For example:

$$K^{p}_{11} = - \frac{\partial F_{ax}}{\partial u_a} = - \frac{1}{2} p \frac{\partial \Delta y}{\partial u_a} = 0$$

$$K^{p}_{12} = - \frac{\partial F_{ax}}{\partial v_a} = - \frac{1}{2} p \frac{\partial \Delta y}{\partial v_a} = \frac{1}{2} p$$

etc.

The interpretation of the follower load is easily recognized as the sum of two contributions as follows: Using element-oriented displacements the follower force matrix for out-of-plane motion is:

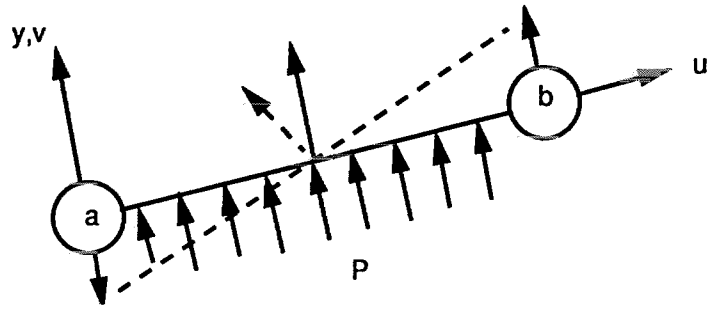

Figure 2. Follower Force for Element Rotation.

$$\begin{Bmatrix} F_{xa} \\ F_{ya} \\ F_{xb} \\ F_{yb} \end{Bmatrix} = \frac{p \cdot \Delta x}{2} \cdot \frac{1}{\Delta x} \begin{bmatrix} 0 & +1 & & -1 \\ & 0 & & \\ & +1 & 0 & -1 \\ & & & 0 \end{bmatrix} \begin{Bmatrix} u_a \\ v_a \\ u_b \\ v_b \end{Bmatrix} \tag{17}$$

The surface increment load change for in-plane motion is simply due to the change in area:

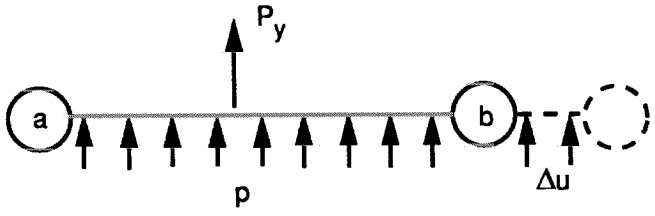

Figure 3. Follower Force for Inplane Motion.

$$\begin{Bmatrix} F_{xa} \\ F_{ya} \\ F_{xb} \\ F_{yb} \end{Bmatrix} = \frac{p}{2} \begin{bmatrix} 0 & & & \\ -1 & 0 & +1 & \\ & & 0 & \\ -1 & & +1 & 0 \end{bmatrix} \begin{Bmatrix} u_a \\ v_a \\ u_b \\ v_b \end{Bmatrix} \tag{18}$$

The complete pressure follower load for a line element is a non-symmetric element matrix

$$\begin{Bmatrix} F_{ax} \\ F_{ay} \\ F_{bx} \\ F_{by} \end{Bmatrix} = \frac{p}{2} \begin{bmatrix} 0 & +1 & & -1 \\ -1 & 0 & +1 & \\ & +1 & 0 & -1 \\ -1 & & +1 & 0 \end{bmatrix} \begin{Bmatrix} u_a \\ v_a \\ u_b \\ v_b \end{Bmatrix} \tag{19}$$

Note that for a continuous multi-element line the diagonal partitions will cancel. The only remaining unsymmetric terms will occur at the ends.

The familiar initial stress differential stiffness matrix for an axial load N is shown below for comparison with the follower load for the same element

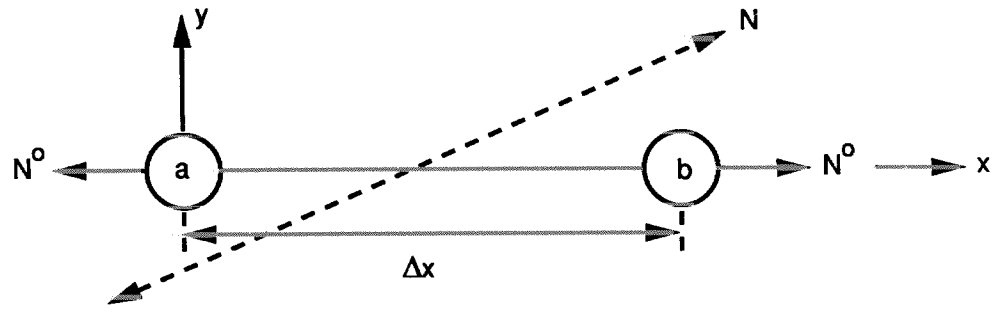

Figure 4. Initial Stress Stiffness.

The Initial Stress Differential Stiffness of an axial load is:

$$\begin{Bmatrix} F_{xa} \\ F_{ya} \\ F_{xb} \\ F_{yb} \end{Bmatrix} = \underbrace{\frac{N}{\Delta x}\begin{bmatrix} 0 & & & \\ & -1 & & +1 \\ & & 0 & \\ & +1 & & -1 \end{bmatrix}}_{K^{\sigma}} \begin{Bmatrix} u_a \\ v_a \\ u_b \\ v_b \end{Bmatrix} \tag{20}$$

The matrix K^{σ} is always symmetric for element loads.

Pressure Follower loads on a polygon

Some of the principles involved in the pressure follower load matrix are now demonstrated on a closed two-dimensional polygon, showing that for uniform pressure the diagonal terms vanish.

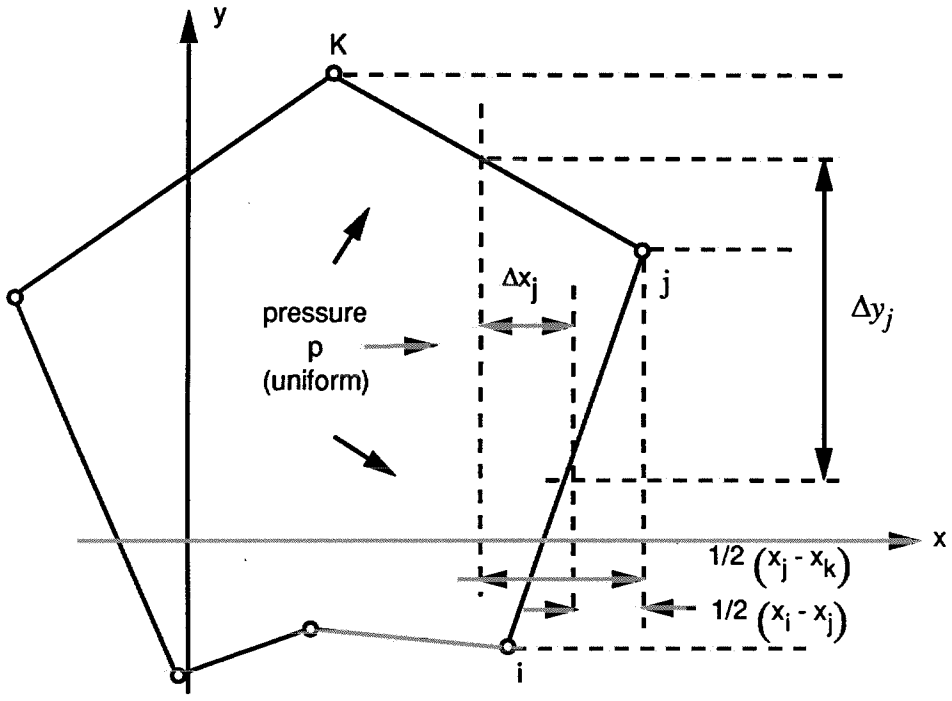

Figure 5. General 2D Follower Force.

Note that the pressure load at node j is independent of the location of j, and only depends on the location of the two adjacent nodes i and k:

$$F_{jx} = p \cdot \Delta z \cdot \frac{1}{2} (y_k - y_i); \quad \delta F_{jx} = \frac{\partial F_{jx}}{\partial y} \cdot \delta_y = \frac{p\Delta z}{2} (\delta_{yk} - \delta_{yi}) \tag{21}$$

$$F_{jy} = p \cdot \Delta z \cdot \frac{1}{2} (x_k - x_i); \quad \delta F_{jy} = \frac{\partial F_{jy}}{\partial x} \cdot \delta_x = \frac{p \cdot \Delta z}{2} (\delta_{xk} - \delta_{xi})$$

Pressure Follower Loads on Three-Dimensional Surfaces

Expanding the preceding two-dimensional case into general three-dimensional form, using a set of triangles enclosing node o as shown in Fig. 6 .

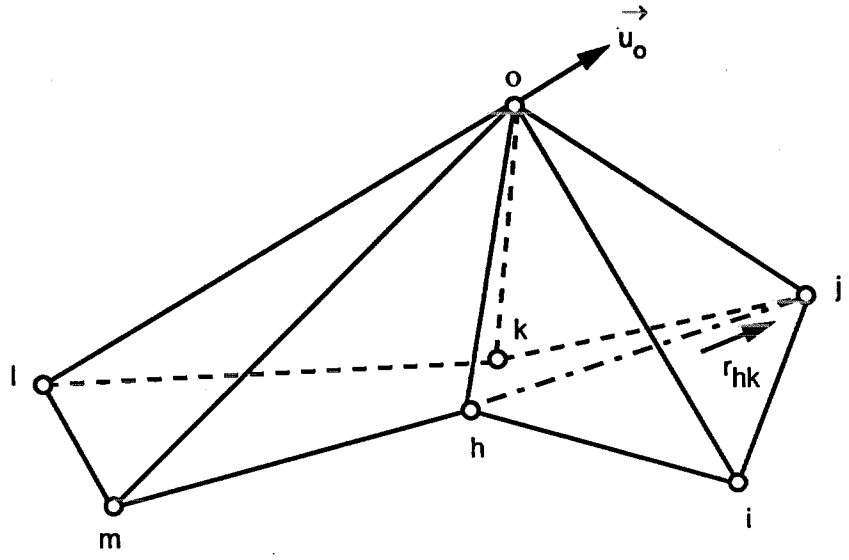

Figure 6. Triangular Surface Facets.

The nodal points o, h, i, ... etc., lie on a general surface. For uniform pressure the net follower load at any enclosed node o is not affected by its own displacement, which will be shown subsequently.

Change of pressure load on a triangle is developed in vector form as follows.

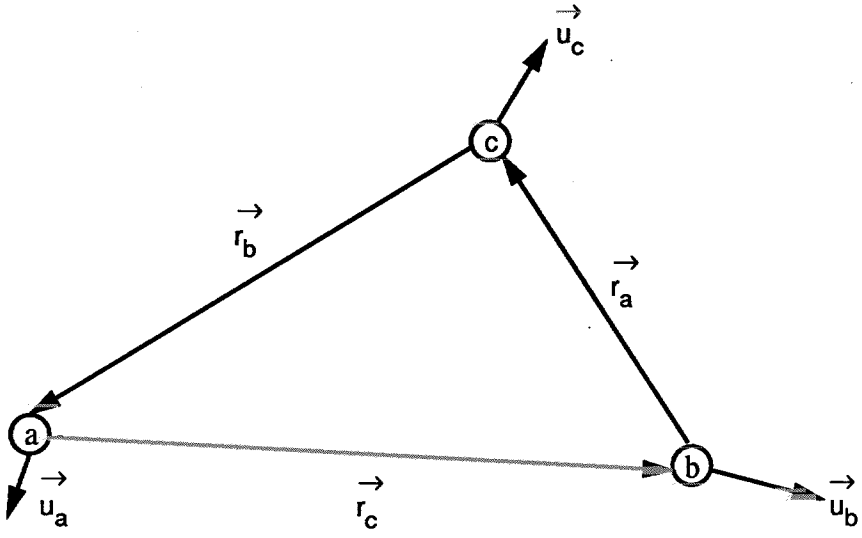

Figure 7. Vectors on a Surface Triangle.

The general nodal displacement vectors $\vec{u}_a$, $\vec{u}_b$, $\vec{u}_c$

where typically, $\vec{u}_a = \{u_a, v_a, w_a\}$

The sides of the triangle will be indexed by the opposite node, typical:

$$\vec{r}_a = \vec{r}_{bc} = \vec{r}_{oc} - \vec{r}_{ob} = \{\Delta x_a, \Delta y_a, \Delta z_a\}^T \qquad (22)$$

The total pressure load vector on the triangle is given by the vector product:

$$\vec{F}_p = p.\vec{A} = \frac{p}{2}(\vec{r}_c \times \vec{r}_a) = \frac{p}{2}(\vec{r}_a \times \vec{r}_b) = \frac{p}{2}(\vec{r}_b \times \vec{r}_c) \qquad (23)$$

Thus the variation in pressure load is determined by the variation of the area vector with the displacements $\vec{u}_a$:

$$2\left(\vec{A} + \delta\vec{A}(a)\right) = \vec{r}_a \times (\vec{r}_b + \vec{u}_a) = \frac{2}{p}\left(\vec{F} + \delta\vec{F}(a)\right) \qquad (24)$$

$$\delta\vec{F}(a) = p \cdot \delta\vec{A}(a) = \frac{p}{2}\vec{r}_a \times \vec{u}_a$$

The total variation of the area vector and pressure force with all nodal displacements is:

$$\frac{2}{p}\delta\vec{F}_p = \vec{r}_a \times \vec{u}_a + \vec{r}_b \times \vec{u}_b + \vec{r}_c \times \vec{u}_c \qquad (25)$$

To Consider the loads on the generally curved surface around a common node, Figure 4, under uniform pressure p, the variation of the force at node o with displacement $\vec{u}_o$ from one triangle (i) is using Equation 25:

$$\delta\vec{F}^i_o(u_o) = \frac{p}{6}\vec{r}_o(i) \times \vec{u}_o \qquad (26)$$

Where $\vec{r}_o(i)$ is the side opposite point "o" for triangle i.

Summarizing all triangles around the central node o:

$$\Sigma\, \delta\vec{F}_o\,(u_o) = \frac{p}{6}\left(\sum_{i=1}^{n} \vec{r}_o(i)\right) \times \vec{u}_o \qquad (27)$$

However, note the vector sum $\Sigma\, \vec{r}_o(i)$ for all triangles is the closed circumferential vector polygon around the central node, thus

$$\Sigma\, \vec{r}_o(i) = 0 \quad \text{and} \quad \Sigma\, \delta\vec{F}_o = 0$$

Thus also for the general curved surface under uniform pressure, the variation in pressure load on a central node (o) with the displacement $\vec{u}_o$ at that node, i.e. the diagonal partition vanishes.

The complete pressure follower matrix for triangle a,b,c is formed, using equation 24 and 25, in terms of both geometry and displacement vectors:

$$\begin{Bmatrix} \vec{F}_a \\ \vec{F}_b \\ \vec{F}_c \end{Bmatrix} = \frac{p}{6} \left[\begin{array}{ccc|ccc|ccc} \vec{r}_a & \times & \vec{u}_a & \vec{r}_b & \times & \vec{u}_b & \vec{r}_c & \times & \vec{u}_c \\ \hline \vec{r}_a & \times & \vec{u}_a & \vec{r}_b & \times & \vec{u}_b & \vec{r}_c & \times & \vec{u}_c \\ \hline \vec{r}_a & \times & \vec{u}_a & \vec{r}_b & \times & \vec{u}_b & \vec{r}_c & \times & \vec{u}_c \end{array}\right] \qquad (28)$$

The vector product $\vec{r}_a \times \vec{u}_a$, typically, is expressed in component form:

$$2\,\vec{\delta A}(a) = \begin{bmatrix} 0 & -\Delta z_a & +\Delta y_a \\ +\Delta z_a & 0 & -\Delta x_a \\ -\Delta y_a & +\Delta x_a & 0 \end{bmatrix} \begin{Bmatrix} u_a \\ v_a \\ w_a \end{Bmatrix} = [X_a]\{u_a\} \tag{29}$$

Introducing the definition of the vector product matrices, $[X_a]$, from Eq. 29, typical, into Eq. 28:

$$\begin{Bmatrix} F_a \\ -- \\ F_b \\ -- \\ F_c \end{Bmatrix} = p_o \left[\begin{array}{c|c|c} X_a & X_b & X_c \\ \hline X_a & X_b & X_c \\ \hline X_a & X_b & X_c \end{array}\right] \begin{Bmatrix} u_a \\ -- \\ u_b \\ -- \\ u_c \end{Bmatrix} = p_o \cdot [K^{po}]\{u\} \tag{30}$$

where $p_o = p/6$.

Closed System Under Uniform Pressure

The assembled pressure follower matrix becomes symmetrical if the structure is a closed system and the pressure is uniform. This can be shown as follows:

A typical coupling term between the common nodes b and d of two adjacent triangles is:

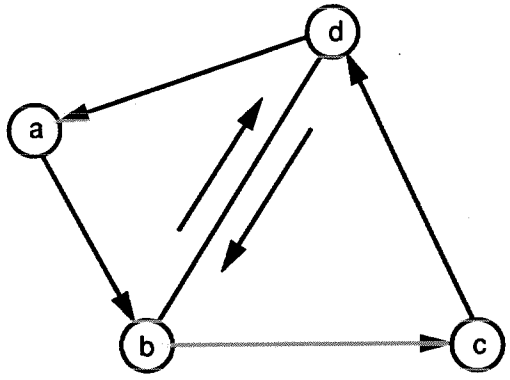

Figure 8. Connected Plates.

$$\vec{F}_b\,(u_d) = \frac{p}{6}\left(\vec{r}_{ab} \times \vec{u}_d + \vec{r}_{bc} \times \vec{u}_d\right) = \frac{p}{6} \cdot \vec{r}_{ac} \times \vec{u}_d = \frac{p}{6}\,[X_{ac}]\{u_d\} \qquad (31)$$

and the reciprocal term is:

$$\vec{F}_d\,(u_b) = \frac{p}{6}\left(\vec{r}_{cd} \times \vec{u}_b + \vec{r}_{da} \times \vec{u}_b\right) = \frac{p}{6}\left(-\vec{r}_{ac} \times \vec{u}_b\right) = -\frac{p}{6}\,[X_{ac}]\{u_b\} \qquad (32)$$

From Eq. (29) we note that $-[X_{ac}]=[X_{ac}]^T$, therefore $\vec{F}_d(u_b)=[X_{ac}]^T\{u_b\}$ and the forces are reciprocal.

Hence for two adjacent triangles the off diagonal terms along the common side are symmetrical if pressure is uniform. And since on a closed system any side satisfies this condition, the resulting matrix is symmetrical.

Pressure Follower Load Element Arch Buckling Test

To demonstrate the effectiveness of the developed pressure follower load matrix for surface elements the classical arch problem under uniform pressure was chosen. The theoretical critical buckling pressure is given on the next page. For the full 180° arch this is a valid bifurcation buckling problem. See Figure 9.

The arch was modeled as a short 1" long cylinder using QUAD4 shell elements. Test parameters were chosen so that the critical eigenvalue for the theoretical buckling pressure should be

$$\lambda_{Th} = 1.0$$

The short cylinder was constrained to ascertain behavior like the theoretical arch.

The model was analyzed using MSC/NASTRAN buckling Solution 5, with increasing mesh density. Two series were run for comparison.

A. With follower load elements.
B. No follower load elements used.

As expected the comparison of the two series demonstrated the effectiveness of the new follower load elements in providing an excellent solution (see Figure 10).

STABILITY OF CIRCULAR ARCH

Hydrostatic uniform pressure

MSC/NASTRAN SOLUTION

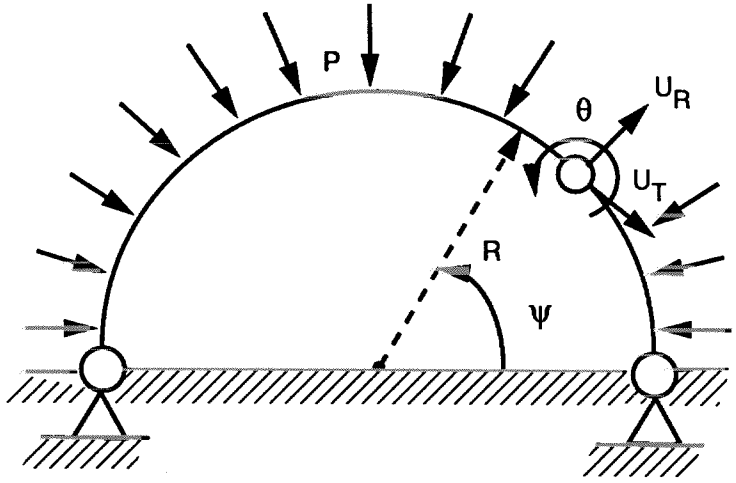

ARCH UNDER HYDROSTATIC PRESSURE

Critical pressure: $P_{CR} = 3EI/R^3$

Data Selection: $p = p_{CR} = 3000$ theoretical value

Thus the theoretical eigenvalue is $\lambda_{Th} = 1.0$

Select $I = p_{CR} \cdot R^3/3E = 3 \cdot 10^3 \cdot 10^3/3 \cdot 10^6$

$R = 10.0$; $E = 10^6$ $I = 1.0$

Hoopload: $P_T = p \cdot R = 30000.- = 3.0E4$

Circumferential grid point spacing $\Delta\psi$ tested:

$\Delta\psi = 30°$

$= 18°$

$= 9°$

$= 4.5°$

Figure 9. Buckling of a Pressurized Arch.

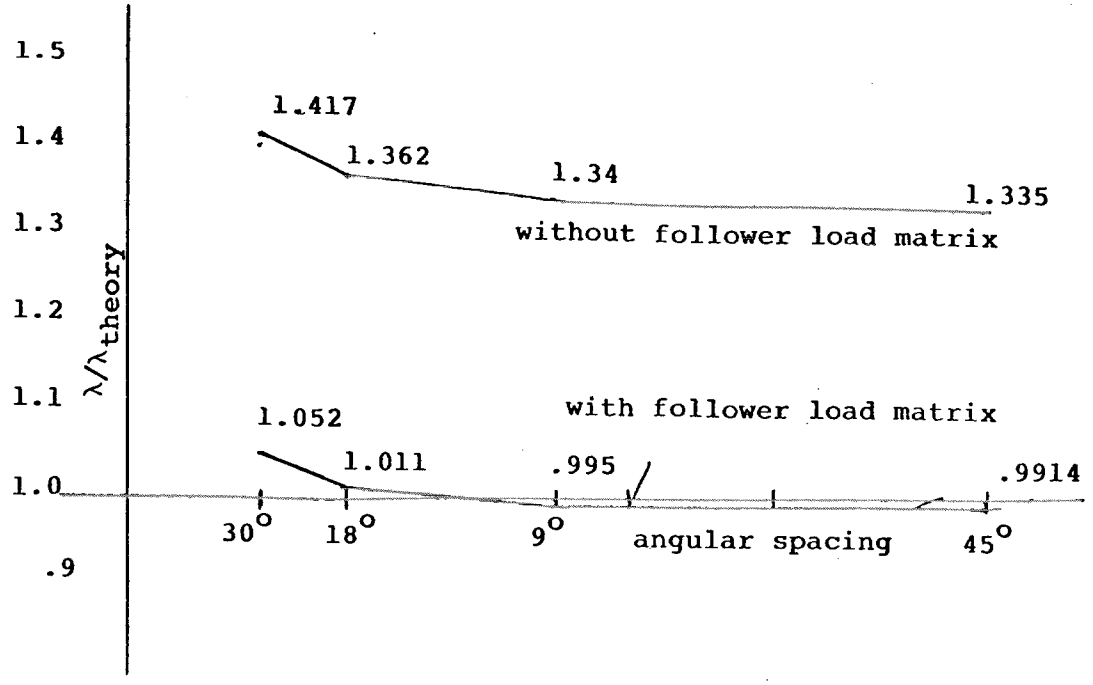

Figure 10. Buckling of Cylinder under Uniform Pressure.

Constraints for arch buckling

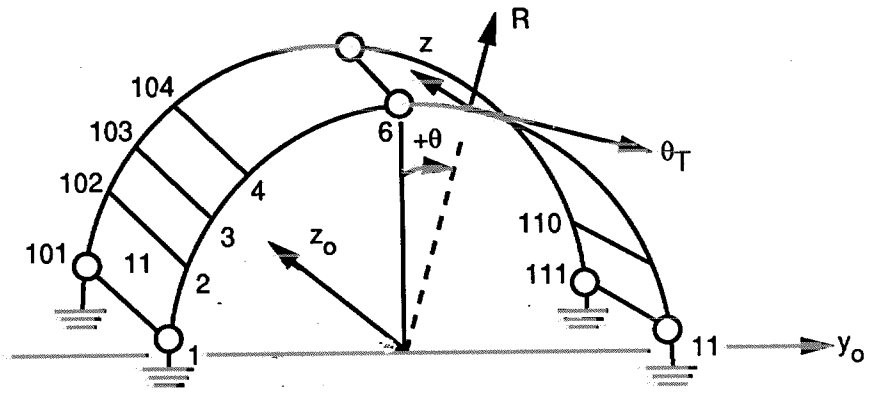

CYLINDRICAL DISPLACEMENT COORDINATE SYSTEM used:

R, T, Z

Generally free DOF: radial, U_1

tangential, U_2

axial rotation, U_6

Constrained at all nodes: $U_Z(U_3)$, $\theta_R(U_4)$, $\theta_T(U_5)$

Plane of Symmetry constraints (plane Y_o, Z_o)

Normal to plane translations: $T(=U_2)$

In plane rotations: $\theta_Z(U_6)$

Figure 11. Constraints for Arch Buckling.

CYLINDER VIBRATION TEST WITH PRESSURE FOLLOWER LOADS

Vibration Test Cyl. Quadrant

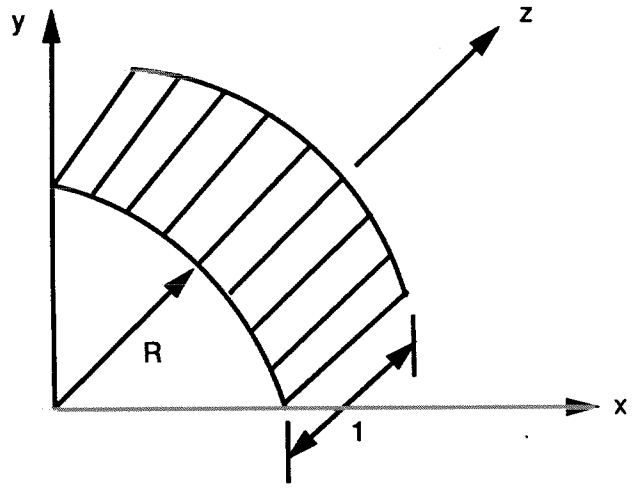

Figure 12. One Quadrant Cylinder Model.

Radius R = 5.0", height = 1"
Thickness t = 0.1"

Material: a) Isotropic $E = 3.0 \times 10^7$ $\nu = .33$ $\rho = 4.28$

Pre-stress static solution with symmetric constraints for all planes.

Vibration modes ASY - ASY at both planes of symmetry (yz and xz planes).

Both ends of the cylinder have the same constraint.

- Eigenvalue Results (New Elements) $\lambda_1 = 6 \times 10^{-4}$
  p = 1000 psi $\lambda_2 = 1 \times 10^2$

- Eigenvalue Results (Standard) $\lambda_1 = 5 \times 10^2$
  $\lambda_2 = 9 \times 10^2$

TABLE 1. BOUNDARY CONSTRAINTS

The boundary constraints on all nodes in the two planes of symmetry are as follows:

• Plane of symmetry →	Plane x,y	Plane z,x
• Symmetric SPC constraints: SYM	$u_z\ \theta_z\ \theta_y$	$u_y\ \theta_x\ \theta_z$
• Antisymmetric SPC constraints: ASY	$u_x\ u_y\ \theta_z$	$u_z\ u_x\ \theta_y$
Static Analysis: Internal pressure (footprint etc.) results in pre-stressed displacements.	SYM	SYM
Vibration Analysis, with static pre-stress		
1) Boundary SPC: SYM, SYM free rigid body modes: u_x	$u_z\ \theta_x\ \theta_y$	$u_y\ \theta_x\ \theta_z$
2) Boundary SPC: SYM, ASY free rigid body modes: u_y, θ_z	$u_z\ \theta_x\ \theta_y$	$u_z\ u_x\ \theta_y$
3) Boundary SPC: ASY, SYM free rigid body modes: u_z, θ_y	$u_x\ u_y\ \theta_z$	$u_y\ \theta_x\ \theta_z$
4) Boundary SPC: ASY, ASY free rigid body modes: θ_x	$u_x\ u_y\ \theta_z$	$u_z\ u_x\ \theta_y$

REFERENCES

1. Schweizerhof, K.; and Ekkehard, R.; " Displacement Dependent Pressure Loads in Nonlinear Finite Element Analyses," Computers & Structures, Vol. 18, No. 6, pp 1099-1114, 1984.

2. Zienkiewicz, O.C.; "The Finite Element Method," 3rd. Edition, Chapter 12, McGraw-Hill U.K., 1977.